












Echeveria subrigida Leaf Extracts Standardized for Isorhamnetin-3-O-Glucoside Show Antidiabetic Effects via the PI3K/Akt Pathway in Rats

Yudith Escobar-Zuñiga ¹, Francisco Delgado-Vargas ¹, José Angel López-Valenzuela ¹, Jesús Ricardo Parra-Unda ¹, José Geovanni Romero-Quintana ¹, Guadalupe Loarca-Piña ², Margarita del Socorro Dávila-Paredes ³, Karen Virginia Pineda-Hidalto ¹, Gabriela López-Angulo ^{1,*}

¹ School of Chemical and Biological Sciences, Autonomous University of Sinaloa, Sinaloa, Mexico

² Research and Graduate Program in Food Science, School of Chemistry, Autonomous University of Queretaro, Queretaro, Mexico

³ School of Veterinary Medicine and Zootechnies, Autonomous University of Sinaloa, Sinaloa, Mexico

*Corresponding Author: School of Chemical and Biological Sciences, Autonomous University of Sinaloa, Sinaloa, Mexico. Email: gabylopez@uas.edu.mx

Received: 4 December, 2024; Revised: 18 January, 2025; Accepted: 29 January, 2025

Abstract

Background: Treatments for type 2 diabetes mellitus (DM2) are not universally effective, underscoring the need for new therapeutic alternatives. Extracts of *Echeveria subrigida* have demonstrated potent in vitro activities, such as antioxidant and α -glucosidase inhibitory effects, as well as in vivo activities, including hypoglycemic, antihyperglycemic, immunomodulatory, and adaptogenic effects.

Objectives: The present study aimed to investigate the antidiabetic mechanisms of ethanolic (EEEs) and methanolic (MEEs) extracts of *E. subrigida*, standardized for isorhamnetin-3-O-glucoside (I3G), in streptozotocin (STZ)-induced diabetic rats.

Methods: The *E. subrigida* extracts, EEEs and MEEs, were obtained by maceration and standardized for the content of I3G. The antidiabetic effect was evaluated using STZ-induced diabetic rats, which were randomly allocated to experimental groups (n = 6). Isorhamnetin (ISO) and metformin (MET) treatments served as positive controls. Parameters were measured at least in triplicate, and means were compared using the Fisher test ($P < 0.05$). The following evaluations were conducted: Levels of monocyte chemoattractant protein-1 (MCP-1), leptin, and inflammatory-related cytokines in serum; expression of proteins in the phosphatidylinositol 3-kinase (PI3K) and adenosine monophosphate-activated protein kinase (AMPK) pathways; transcriptional expression of peroxisome proliferator-activated receptor alpha (PPAR α) and sterol regulatory element-binding protein 1c (SREBP-1c) in liver tissue; and histology of the liver and pancreas.

Results: All treatments, except ISO, demonstrated antidiabetic effects, with glucose levels in MET (183.75 ± 61.89 mg/dL) and MEEs (168.00 ± 48.10 mg/dL) rats comparable to healthy control (HC) rats (109.25 ± 6.11 mg/dL). Leptin levels decreased in diabetic control (DC) rats (0.17 ± 0.07 ng/mL), while levels in the EEEs (0.65 ± 0.06 ng/mL) and MEEs (0.77 ± 0.09 ng/mL) groups were similar to those of the HC group (0.71 ± 0.19 ng/mL). The levels (pg/mL) of cytokines (IL-10, IL-6, IFN- γ , and IL-4) were elevated in DC rats (72.26 ± 12.91 , 36.72 ± 2.91 , 4.56 ± 0.63 , and 16.34 ± 2.06 , respectively), but were effectively reduced in rats treated with EEEs (29.64 ± 2.86 , 9.85 ± 2.92 , 1.11 ± 0.24 , and 6.71 ± 1.15 , respectively) and MEEs (26.65 ± 5.31 , 7.30 ± 1.89 , 1.25 ± 0.28 , and 5.55 ± 0.43 , respectively). Liver histology showed nearly normal structures, although pancreatic histology revealed hypertrophied Langerhans islets across all DM2 groups. The Akt activation and inactivation of AS160 by phosphorylation were detected in the livers of EEEs and MEEs rats without AMPK activation. Additionally, these groups expressed the SREBP-1c mRNA.

Conclusions: The EEEs and MEEs exhibited antidiabetic activity via the PI3K/Akt pathway, suggesting *E. subrigida* as a potential preventive or therapeutic agent for type 2 diabetes.

Keywords: Diabetes, Antidiabetic Mechanism, PI3K/Akt Pathway, Crassulaceae, Leptin, Cytokines

1. Background

Type 2 diabetes mellitus (DM2) is a disease characterized by hyperglycemia. Untreated DM2

patients develop severe damage to organs and systems, resulting in complications such as cardiac failure, retinopathy, and neuropathy (1, 2). The primary

mechanism of insulin in regulating glucose and lipid metabolism involves the phosphatidylinositol 3-kinase (PI3K) pathway, which is compromised in DM2 patients (3, 4). Under stress conditions (e.g., physical exercise and prolonged fasting), glucose assimilation is associated with the adenosine monophosphate-activated protein kinase (AMPK) pathway. Therefore, regulating this pathway is crucial for preventing and treating diabetes (4, 5). The etiology of diabetes has been linked to inflammation. Chronic high glucose concentration produces metabolites that increase the levels of proinflammatory cytokines, inducing low insulin sensitivity, hyperinsulinism, and diabetes. Consequently, modulating proinflammatory cytokine levels is a strategy for preventing and treating diabetes (4, 6). Leptin levels are also associated with obesity and diabetes, and this parameter is decreased in DM2 patients (7, 8). Current commercial treatments for diabetes have not shown sufficient efficacy, highlighting the need for new therapies. In this context, plant flavonoids have been shown to improve glucose assimilation and metabolism, including hesperetin, luteolin, catechin, genistein, quercetin, and kaempferol (6). For example, a *Wisteria sinensis* extract enriched in luteolin and apigenin derivatives improved glucose metabolism in diabetic rats (9). Our research group demonstrated that the methanol extract of *Echeveria subrigida* (B.L. Rob. & Seaton) rose leaves has high in vitro antioxidant activity, and the main phenolics present in the extract were isorhamnetin (ISO), quercetin, and kaempferol derivatives (10, 11). The α -glucosidase inhibitory activity of the same extract (IC_{50} 25.21 - 50.57 μ g/mL) was stronger than that of acarbose (IC_{50} 3.59 mg/mL), suggesting its potential as an antidiabetic agent (12). Fractionation of the methanol extract of *E. subrigida* identified isorhamnetin-3-O-glucoside (I3G) (IC_{50} = 166.4 μ g/mL), quercetin-3-O-glucoside (Q3G) (IC_{50} = 131.1 μ g/mL), and tannins (IC_{50} = 9.6 μ g/mL) as the primary compounds responsible for the α -glucosidase inhibition (13). A hydroalcoholic extract of *E. subrigida* leaves showed high adaptogenic and immunomodulatory activities, which could contribute to its antidiabetic effects (14). Based on these studies, an I3G-standardized hydroalcoholic extract of *E. subrigida* leaves was prepared, and an in vivo assay with normoglycemic mice showed significant hypoglycemic and antihyperglycemic effects (15). These results support the antidiabetic potential of the I3G-standardized

hydroalcoholic extract of *E. subrigida*. These effects could be due to activation of the PI3K and AMPK pathways.

2. Objectives

The aim of this study was to investigate the antidiabetic mechanisms of ethanolic (EEEs) and methanolic (MEEs) extracts of *E. subrigida*, standardized for I3G, in streptozotocin (STZ)-induced diabetic rats.

3. Methods

3.1. Chemicals

The reagents were purchased from Sigma Aldrich (St. Louis, MO, USA), and HPLC solvents were obtained from TEDIA (Fairfield, OH, USA).

3.2. Plant Material and Preparation of the Ethanolic and Methanolic Extracts

Leaves of *E. subrigida* rose (B. L. Rob. & Seaton) were collected near the town of El Palmito, Concordia, Sinaloa (2,000 m above sea level; N 23° 34' 06", W 105° 50' 53"; Vega-Aviña R.; 11742) in November 2019. They were transported to the Laboratory of Chemistry of Natural Products, School of Chemical and Biological Sciences, Autonomous University of Sinaloa. The *E. subrigida* leaves were freeze-dried (VirTis 25EL, VirTis Co., Gardiner, NY, USA), milled, and passed through a number 40 mesh. The powder (100 g) was mixed with methanol (1:10 w/v) to obtain the MEEs or with 80% ethanol (1:10 w/v) to obtain the EEEs. The extraction was carried out for three days with daily solvent exchange. The solvent was removed at 40°C using a rotary evaporator (BÜCHI Labortechnik AG, Switzerland), followed by the removal of any residual solvent from EEEs in a vacuum oven (Thermo Scientific™, Waltham, MA, USA) at 40°C. Finally, both MEEs and EEEs samples were freeze-dried. Both extracts were stored at -20°C in darkness until use.

3.3. Determination of Isorhamnetin-3-O-Glucoside by HPLC

The concentrations of I3G, Q3G, and tannins in the extracts were quantified by HPLC analysis using an ACCELA HPLC-DAD (Thermo Scientific, USA) equipped with an ACE EXCEL C18 - Amide column (150 × 30 mm × 3 μ m) (Advanced Chromatography Technologies, UK) as described by Heredia-Mercado et al. (15). The mobile phase consisted of 1% formic acid (A) and acetonitrile (B): 0.5% B, linear gradient to 16% B in 4 minutes, linear gradient to 60% B in 17 minutes, and isocratic for 5

minutes. The separation conditions were as follows: Operating time of 35 minutes, flow rate of 0.3 mL/min, injection volume of 15 μ L, and detection at 280, 320, and 350 nm. For the HPLC analysis, 100 mg of extract was dissolved in 10 mL of methanol; a 1:1 dilution was prepared, passed through a PVDF filter (17 mm, 0.45 μ m, TITAN, USA), and injected. Flavonoids were measured using calibration curves of I3G and Q3G, and tannins were quantified using a calibration curve of catechin; values were reported as milligrams of compound per gram of extract. It was previously reported that the standardized extracts of *E. subrigida* leaves contain at least 4.82 mg of I3G or 3.01 mg of Q3G per gram (16).

3.4. Animals

Six-week-old male Wistar rats were used. The animals were kept in the FCQB-UAS vivarium at 24°C, 50% humidity, and 12-hour light-dark cycles. They were fed a standard diet containing 3% fat, 49% carbohydrates, 23% protein, 6% fiber, 7% ash, and 12% moisture (Nutricubos, Nutrimentos Purina S.A. de C.V., Mexico). The research was conducted in accordance with the Official Mexican Standard NOM-062-ZOO-1999.

3.5. Animal Experimental Design

The rats underwent a 7-day adaptation period with a regular diet. After this period, the animals were provided with a 10% sucrose solution instead of drinking water for 15 days. They then fasted for seven hours (7:00 a.m. to 2:00 p.m.) with free access to water, and diabetes was induced by intraperitoneal (i.p.) administration of STZ [50 mg/kg body weight (b.w.)]. The STZ was resuspended in cold citrate buffer (0.1 M citric acid, pH 4.5) prepared at the time of application, and the animals were injected within the following 5 minutes. Thirty minutes later, rats were provided with a 5% sucrose solution instead of drinking water for 48 hours to prevent hypoglycemia and death. Control rats received an equivalent i.p. dose of the citrate buffer used as a vehicle (pH 4.5, 10 mL/kg b.w.). One week after injection, glucose levels were measured in blood sampled from the tail using an Accu-Chek® instant glucometer. Rats with blood glucose levels higher than 200 mg/dL were considered to have DM2 (17) and were used for experimentation. Six groups of animals (n = 6) were formed: Healthy control (HC); diabetic control (DC); MET: Diabetic + metformin treatment (500 mg/kg b.w.); ISO: Diabetic + isorhamnetin (1.9 mg/kg b.w.); EEEs: Diabetic + *E. subrigida* ethanolic extract (400 mg/kg

b.w.); and MEEs: Diabetic + *E. subrigida* methanolic extract (284.7 mg/kg b.w.). The employed doses of ISO, EEEs, and MEEs were adjusted to provide the same quantity of ISO. Oral treatments were administered once a day (17:30 h) for 30 days. Body weight and blood glucose levels were measured at the start of the experiment and weekly.

At the end of the experiment, rats were euthanized following the Mexican Official Norm NOM-062-ZOO-1999. The animals were anesthetized with ether, and blood was collected by cardiac puncture in polystyrene tubes without anticoagulant (BD Vacutainer®). Subsequently, manual cervical dislocation was performed. Serum was immediately recovered by centrifugation (PowerSpin™ MX Centrifuge, UNICO, Chicago, IL, USA) at 2500 rpm at room temperature for 10 minutes. Animals were dissected to obtain the liver and pancreas. Portions of the liver and pancreas were sliced, fixed, and stained for histological analysis. The remaining liver tissue was frozen with liquid nitrogen until processing.

3.6. Oral Glucose Tolerance Test

On day twenty-one of treatment, an oral glucose tolerance test was performed after a 6-hour daytime fast. Blood was drawn to measure basal glucose, and then treatments were administered. Thirty minutes later, an oral sucrose load of 3.0 g/kg body weight (b.w.) was administered. Blood was obtained by tail puncture after 30, 60, and 120 minutes to measure glucose using an Accu-Chek® instant glucometer.

3.7. MCP-1 and Leptin Analysis

Serum levels of monocyte chemoattractant protein-1 (MCP-1) (PicoKine™ ELISA) and leptin (no. RAB0335, Sigma-Aldrich, USA) were analyzed using ELISA kits according to the manufacturer's protocols. Three biological replicates were measured per duplicate: Rats in each experimental group were randomly allocated into groups of two, and their sera were mixed to measure the MCP-1 and leptin levels.

3.8. Cytokine Analysis

The levels of IL-4, IL-6, IL-10, IL-17A, and IFN- γ were analyzed using a flow cytometer (BD Accuri C6, USA) with the commercial Th1/Th2/Th17 kit (catalog number 560485; BD Bioscience-Pharmingen) according to the manufacturer's instructions. The analysis was carried

out in triplicate, as indicated in section 3.7. The level of each cytokine was measured using the corresponding standard curve.

3.9. Liver and Pancreas Histology

Liver and pancreas slices were fixed in 4% formaldehyde, embedded in paraffin, and stained with hematoxylin-eosin (HE) (TissuePro Technology, Gainesville, FL, USA). The stained tissues were observed with an optical microscope (Nikon ECLIPSE E200, Nikon Instruments Inc., Melville, NY, USA) at 40× magnification.

3.10. Analysis of Proteins from the PI3K and AMPK Pathways

The levels of expression and phosphorylation of proteins from the PI3K and AMPK pathways were analyzed by Western blot. The analysis was performed with pooled livers from each group; three extractions were carried out and analyzed in duplicate. Proteins from the liver samples were extracted by sonication for 30 minutes in an ice bath using the RIPA kit (Thermo Scientific™ Buffer RIPA Pierce™) containing the protease and phosphatase inhibitors cocktail (Halt™, 100X). The samples were centrifuged (Eppendorf 5417R, Fairfield, OH, USA) at 12,000 × g for 15 minutes at 4°C, and the supernatant was recovered (9). Protein concentration was determined with the BCA kit (Pierce™ BCA Protein Assay Kit) and adjusted to 60 µg/µL. Proteins were separated by SDS-PAGE and transferred to a nitrocellulose membrane (Hybond™-ECL™ Amersham Biosciences). The membrane was blocked with 5% non-fat milk proteins (Svelty, Nestle®) and incubated for 2 hours with a primary monoclonal antibody (Cell Technology Inc., Williamsburg, VA, USA): The p-Akt (1:1000), Akt (1:1000), p-AMPKα (1:1000), AMPKα (1:1000), p-AS160 (1:1000), or AS160 (1:1000). Glyceraldehyde 3-phosphate dehydrogenase (GAPDH) (1:1000) was used as an expression control. Membranes were then incubated for 90 minutes with the secondary antibody conjugated with horseradish peroxidase (1:1000). The membranes were treated with 3,3'-diaminobenzidine (Research Organics), and protein band images were analyzed with a ChemicDoc XRS photodocumentation system (Bio-Rad, Hercules, CA, USA) (18).

3.11. Transcriptional Expression of PPARα and SREBP-1c

The mRNA expression was measured with the pooled livers of each group; three extractions were carried out

and analyzed in duplicate. Liver RNA was obtained using the Trizol method, and its quantity and quality were assessed using a spectrophotometer (Nanodrop™ Lite Thermo Scientific™). RNA was converted to cDNA using the iScript IV First-Strand cDNA Synthesis kit (ABP Biosciences, Rockville, MD, USA). The cDNA was used with the One Taq RT-PCR kit (NEW ENGLAND BioLabs® Inc., Ipswich, MA, USA) to determine the expression level of the genes for peroxisome proliferator-activated receptor alpha (PPARα) and sterol regulatory element binding protein (SREBP-1c). Glyceraldehyde 3-phosphate dehydrogenase was used as a housekeeping gene to normalize the mRNA levels of target gene expression. Primers were designed using the UGENE and NCBI Primer-BLAST programs (Table 1). A 2720 thermal cycler (Applied Biosystems™, Foster City, CA, USA) was used, and the running conditions included initial denaturation at 95°C for 30 seconds, followed by 35 cycles at 94°C for 15 seconds, 60°C for 35 seconds, and 72°C for 40 seconds.

3.12. Statistical Analysis

Evaluations were carried out at least in triplicate, and the data are reported as mean ± SD. The normality of data distribution was assessed by the Shapiro-Wilk Test. A one-way ANOVA was used, and the means were compared by Fisher's Test ($P \leq 0.05$). All analyses were carried out using StatGraphics Centurion XVI.I (Statistical Graphics Corporation™, USA).

4. Results

4.1. Flavonoid and Tannins Composition of the *Echeveria subrigida* Extracts

The contents of Q3G, I3G, and tannins (as equivalents of catechin) (mg per gram of dry extract) in the *E. subrigida* extracts were as follows: The EEs, 3.30 ± 0.073 , 4.76 ± 0.201 , 2.70 ± 0.150 ; and MEs, 5.01 ± 0.187 , 6.67 ± 0.201 , 46.36 ± 2.116 . The peak purities of Q3G (999.36) and I3G (998.69) indicated good separation (> 990), while the peak of tannins resulted in a mixture of compounds with a value of 977.08 (Figure 1).

4.2. Body Weight

The body weight gain of the diabetic rat groups (DC, MET, EEs, MEs, and ISO) over four weeks was lower than that of the HC group (Table 2). At the end of the experiment, the gain percentage of the diabetic groups

Table 1. Primers Used for PCR Analysis of Gene Expression in Rat Liver

Genes	Forward Sequence 5'→3'	Reverse Sequence 5'→3'
PPAR α	CCATCTGTCCTCTCTCCCA	TGATGACAGAGCCCTCCGAG
SREBP-1c	AAGATGTACCCGTCCTGCC	CAGGCTTGAGTACCCAGCA
GAPDH	GCTGAGAATGGGAAGCTGGT	GGCGGAGATGATGACCCTTT

Abbreviations: PPAR α , peroxisome proliferator-activated receptor alpha; SREBP-1c, sterol regulatory element binding protein; GAPDH, glyceraldehyde 3-phosphate dehydrogenase.

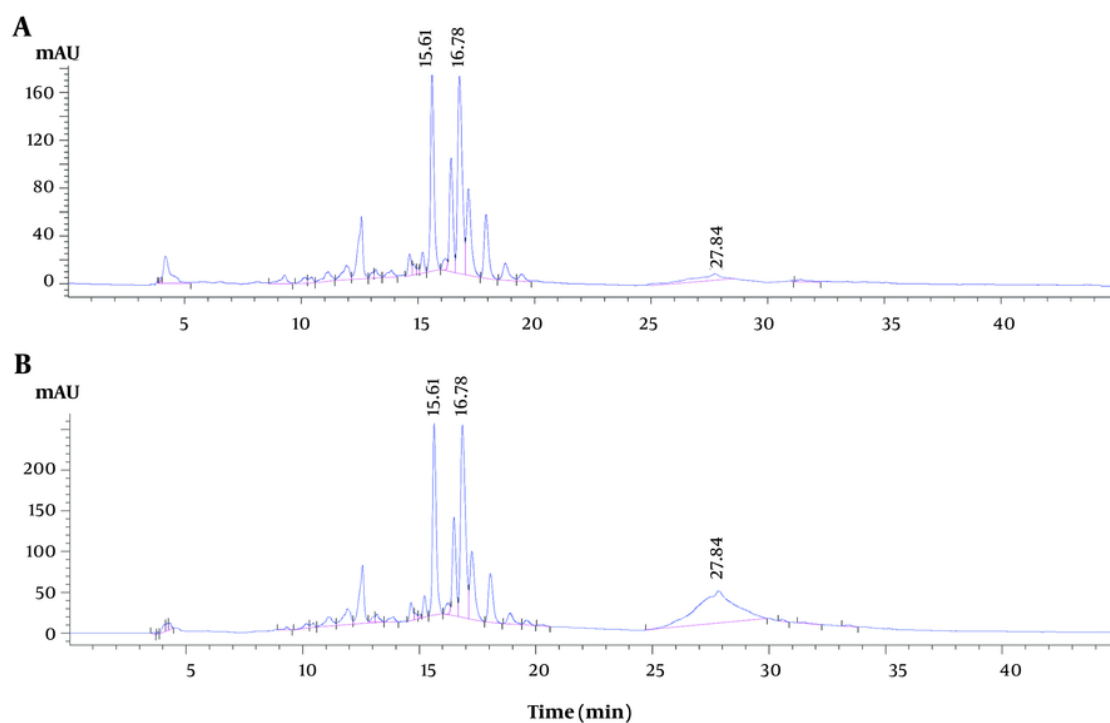


Figure 1. HPLC chromatogram of the ethanolic (A), and methanolic (B) extracts (EEEs and MEEs) of *Echeveria subrigida*. The compounds associated with the hypoglycemic effect (retention time and peak purity) are quercetin-3-O-glucoside (Q3G) (15.61 min, 999.36), isorhamnetin-3-O-glucoside (I3G) (16.78 min, 998.69), and tannins (27.84 min, 977.08).

(18% - 39%) was lower ($P < 0.05$) than that of the HC group (59%).

4.3. Glucose Levels

The rats in the HC group maintained normal glucose levels (96.25 - 109.25 mg/dL) throughout the experiment. At the start of the experiment, DM2 rats had fasting glucose levels higher than 200 mg/dL (Table 3) and exhibited signs of polydipsia, polyphagia, and polyuria, meeting the criteria for inclusion in the study. All treatments, except for the DC and ISO groups, decreased

glucose levels in the DM2 rats, with values for the MET and MEEs groups similar to those of the HC group during the experiment, whereas the EEEs group reached similar values by the fourth week (Table 3).

4.4. Glucose Tolerance Test

Rats in the HC, EEEs, and MEEs groups showed a hyperglycemic peak 30 minutes after the sucrose load (Table 4), and their glucose levels decreased, reaching statistically similar values after 120 minutes. At the same

Table 2. Effect of *Echeveria subrigida* Extracts on the Body Weight of Diabetic Rats ^{a, b, c}

Groups	Weeks of Treatment				
	Initial	1st	2nd	3rd	4th
HC	244.63 ± 15.66 ^{aD}	329.50 ± 17.18 ^{aC}	357.00 ± 24.18 ^{aB}	377.67 ± 23.77 ^{aAB}	385.67 ± 28.38 ^{aA}
DC	245.73 ± 14.43 ^{aC}	288.83 ± 24.30 ^{cdB}	288.00 ± 11.73 ^{dB}	308.17 ± 15.56 ^{cdA}	308.83 ± 11.65 ^{cdA}
MET	243.00 ± 14.99 ^{aC}	308.33 ± 19.04 ^{bb}	324.00 ± 27.09 ^{baB}	339.83 ± 26.59 ^{ba}	336.67 ± 31.21 ^{baB}
ISO	244.88 ± 4.97 ^{aC}	274.00 ± 9.17 ^{dB}	293.83 ± 22.12 ^{cdA}	302.50 ± 12.55 ^{cdA}	290.50 ± 16.40 ^{dAB}
EEEs	244.50 ± 14.15 ^{aD}	297.67 ± 5.57 ^{bcC}	313.17 ± 7.39 ^{bcB}	318.50 ± 6.25 ^{bcAB}	325.17 ± 7.28 ^{bcA}
MEEs	252.00 ± 12.39 ^{aB}	285.50 ± 13.53 ^{cdA}	296.83 ± 15.28 ^{cdA}	296.33 ± 19.76 ^{dA}	301.67 ± 22.03 ^{cdA}

Abbreviations: HC, healthy control; DC, diabetic control; SD, standard deviation ; MET, metformin; ISO, isorhamnetin; EEEs, ethanol extract of *Echeveria subrigida*; MEEs, methanol extract of *E. subrigida*.

^a Values are expressed as mean ± SD (n = 6).

^b Different lowercase letters in the same column and uppercase letters in the same row represent significant differences (Fisher, P < 0.05).

^c MET: Diabetic + MET (500 mg/kg b.w.); ISO: Diabetic + ISO (1.9 mg/kg b.w.); EEEs: Diabetic + EEEs (400 mg/kg b.w.); MEEs: Diabetic + MEEs (284.7 mg/kg b.w.).

Table 3. Effect of *Echeveria subrigida* Extracts on the Blood Glucose Levels of Diabetic Rats ^{a, b, c}

Groups	Weeks of Treatment				
	Initial	1st	2nd	3rd	4th
HC	102.63 ± 5.55 ^{bb}	108.00 ± 5.73 ^{dAB}	96.25 ± 7.23 ^{cc}	105.63 ± 4.17 ^{cAB}	109.25 ± 6.11 ^{ba}
DC	275.25 ± 63.30 ^{aBC}	254.13 ± 60.99 ^{abC}	334.00 ± 69.90 ^{aAB}	354.88 ± 44.60 ^{aA}	315.53 ± 65.18 ^{aAB}
MET	312.00 ± 50.25 ^{aA}	161.75 ± 59.74 ^{cdB}	163.38 ± 72.85 ^{bcB}	147.50 ± 57.36 ^{bcB}	183.75 ± 61.89 ^{bb}
ISO	306.63 ± 53.54 ^{aA}	314.88 ± 124.86 ^{aA}	354.50 ± 121.90 ^{aA}	313.63 ± 139.19 ^{aA}	313.63 ± 139.19 ^{aA}
EEEs	269.75 ± 24.01 ^{aA}	218.25 ± 79.12 ^{bcAB}	202.00 ± 39.84 ^{bbc}	181.25 ± 59.50 ^{bbc}	150.13 ± 39.04 ^{bc}
MEEs	310.60 ± 46.10 ^{aA}	174.20 ± 71.57 ^{bcdB}	153.20 ± 31.55 ^{bcB}	146.80 ± 44.91 ^{bcB}	168.00 ± 48.10 ^{bb}

Abbreviations: HC, healthy control; DC, diabetic control; SD, standard deviation ; MET, metformin; ISO, isorhamnetin; EEEs, ethanol extract of *Echeveria subrigida*; MEEs, methanol extract of *E. subrigida*.

^a Values are expressed as mean ± SD (n = 6).

^b Different lowercase letters in the same column and uppercase letters in the same row represent significant differences (Fisher, P < 0.05).

^c MET: Diabetic + MET (500 mg/kg b.w.); ISO: Diabetic + ISO (1.9 mg/kg b.w.); EEEs: Diabetic + EEEs (400 mg/kg b.w.); MEEs: Diabetic + MEEs (284.7 mg/kg b.w.).

time, the MET group also showed a decrease in glucose levels but did not reach the levels of the HC group.

4.5. Leptin in Serum

At the end of the experiment, the serum leptin levels of the DM2 groups, except for MEEs (0.77 ng/mL), were lower than those of the HC group (0.71 ng/mL) (P < 0.05). The leptin levels of the EEEs group (0.650 ng/mL) were closest to that of the HC group (0.71 ng/mL). Remarkably, the *Echeveria* extracts (MEEs and EEEs) were more effective than MET in improving leptin levels (Table 5).

4.6. Pro- and Anti-inflammatory Molecules

Compared with the cytokine levels (IL-10, IL-17A, IFN- γ , IL-6, IL-4, and MCP-1) in the HC group, the levels of these

molecules in the DC group increased significantly, except for IL-17A levels, which did not change (Table 6). In contrast, the cytokine levels in the *Echeveria*-treated groups (EEEs and MEEs) decreased significantly, except for MCP-1, whose level was similar to that of the DC group. The cytokine levels in the ISO group were significantly higher than those in the HC group, but MCP-1 levels were similar (Table 6). On the other hand, the cytokine levels of the HC and MET groups were statistically similar, except for those of MCP-1, which were lower in the MET group (Table 6).

4.7. Histology Analysis

4.7.1. Pancreas Tissue

Table 4. Oral Glucose Tolerance Test for Diabetic Rats Treated with *Echeveria subrigida* Extracts ^{a, b, c}

Groups	Minutes			
	Initial	30	60	120
HC	101.75 ± 4.68 ^{cBC}	116.75 ± 12.15 ^{cA}	107.75 ± 10.11 ^{cB}	97.75 ± 5.26 ^{cC}
DC	331.43 ± 84.51 ^{aAB}	352.44 ± 92.50 ^{aA}	368.90 ± 127.45 ^{aA}	227.22 ± 123.52 ^{abB}
MET	201.67 ± 87.65 ^{bAB}	230.83 ± 92.63 ^{bAB}	308.22 ± 128.60 ^{aA}	205.00 ± 82.96 ^{abB}
ISO	315.00 ± 116.17 ^{aA}	373.00 ± 152.47 ^{aA}	376.75 ± 144.68 ^{aA}	286.75 ± 162.18 ^{aA}
EEEs	169.17 ± 70.62 ^{bcAB}	226.92 ± 75.87 ^{bA}	209.46 ± 83.63 ^{bA}	148.50 ± 61.12 ^{bcB}
MEEs	159.20 ± 25.39 ^{bcA}	223.17 ± 59.70 ^{bA}	191.33 ± 51.43 ^{bcA}	181.67 ± 62.76 ^{bcA}

Abbreviations: HC, healthy control; DC, diabetic control; SD, standard deviation; MET, metformin; ISO, isorhamnetin; EEEs, ethanol extract of *Echeveria subrigida*; MEEs, methanol extract of *E. subrigida*.

^a Values are expressed as mean ± SD (n = 6).

^b Different lowercase letters in the same column and uppercase letters in the same row represent significant differences (Fisher, P < 0.05).

^c MET: Diabetic + MET (500 mg/kg b.w.); ISO: Diabetic + ISO (1.9 mg/kg b.w.); EEEs: Diabetic + EEEs (400 mg/kg b.w.); MEEs: Diabetic + MEEs (284.7 mg/kg b.w.).

Table 5. Effect of the Treatment with *Echeveria subrigida* Extracts on the Serum Leptin Levels of Diabetic Rats ^{a, b, c}

Groups	Leptin (ng/mL)
HC	0.71 ± 0.19 ^A
DC	0.17 ± 0.07 ^D
MET	0.32 ± 0.05 ^C
ISO	0.38 ± 0.05 ^C
EEEs	0.65 ± 0.06 ^B
MEEs	0.77 ± 0.09 ^A

Abbreviations: HC, healthy control; DC, diabetic control; SD, standard deviation; MET, metformin; ISO, isorhamnetin; EEEs, ethanol extract of *Echeveria subrigida*; MEEs, methanol extract of *E. subrigida*.

^a Values are expressed as mean ± SD (n = 6).

^b Uppercase letters represent significant differences (Fisher, P < 0.05).

^c MET: Diabetic + MET (500 mg/kg b.w.); ISO: Diabetic + ISO (1.9 mg/kg b.w.); EEEs: Diabetic + EEEs (400 mg/kg b.w.); MEEs: Diabetic + MEEs (284.7 mg/kg b.w.).

Streptozotocin treatment damages pancreatic cells and induces diabetes. The pancreas slices of the HC and DM2 (DC, MET, ISO, EEEs, and MEEs) groups showed normal acinar cells. However, the Langerhans islets of the DM2 groups showed hypertrophy, characterized by irregular islet contours and smaller sizes than those of the HC group (Figure 2).

4.7.2. Liver Tissue

The hepatic parenchyma of all groups showed normal structure and absence of steatosis; the size and appearance of the central veins and hepatic sinusoids were similar among groups. However, the sinusoids in the ISO group were dilated (Figure 3).

4.8. Effect of the *Echeveria* Extracts on the PI3K Pathway in the Liver

The Western blot of hepatic protein extracts from all groups detected Akt, whereas the activated phosphorylated form (p-Akt) was present only in the ISO, EEEs, and MEEs groups. In the signaling cascade of Akt, p-Akt inactivates AS160 by phosphorylation (p-AS160). All groups expressed AS160 and p-AS160, but bands were better observed in the DC, MET, and ISO groups (Figure 4).

4.9. Effect of the *Echeveria* Extracts on the AMPK Pathway Activation in the Liver

All groups of rats expressed AMPK, with higher levels observed in the DC, MET, and ISO groups. The activated phosphorylated form (p-AMPK) was detected in the HC, DC, MET, and ISO groups but not in those treated with *Echeveria* extracts (EEEs and MEEs) (Figure 4).

Table 6. Anti- and Pro-inflammatory Cytokines in Diabetic Rats Treated with *Echeveria subrigida* Extract^{a, b, c}

Groups	Cytokines (pg/mL)					
	IL-10	IL-17A	IFN γ	IL-6	IL-4	MCP-1
HC	47.77 ± 12.15 ^B	4.60 ± 0.14 ^C	2.72 ± 0.55 ^C	18.00 ± 3.46 ^C	9.74 ± 0.58 ^B	82.01 ± 15.89 ^{BC}
DC	72.26 ± 12.91 ^A	4.50 ± 0.55 ^C	4.56 ± 0.63 ^B	36.72 ± 2.91 ^A	16.34 ± 2.06 ^A	131.66 ± 34.24 ^A
MET	40.87 ± 10.80 ^{BC}	6.51 ± 1.03 ^B	2.59 ± 0.13 ^C	16.29 ± 2.66 ^C	9.25 ± 1.20 ^B	32.96 ± 21.38 ^D
ISO	72.21 ± 7.15 ^A	14.27 ± 1.22 ^A	6.18 ± 0.41 ^A	28.12 ± 1.64 ^B	15.70 ± 0.63 ^A	70.44 ± 26.32 ^C
EEEs	29.64 ± 2.86 ^C	2.69 ± 0.82 ^D	1.11 ± 0.24 ^D	9.85 ± 2.92 ^D	6.71 ± 1.15 ^C	116.51.0 ± 31.18 ^{AB}
MEEs	26.65 ± 5.31 ^C	1.20 ± 0.60 ^E	1.25 ± 0.28 ^D	7.30 ± 1.89 ^D	5.55 ± 0.43 ^C	143.90 ± 33.85 ^A

Abbreviations: HC, healthy control; DC, diabetic control; SD, standard deviation; MET, metformin; ISO, isorhamnetin; EEEs, ethanol extract of *Echeveria subrigida*; MEEs, methanol extract of *E. subrigida*.

^a Values are expressed as mean ± SD (n = 6).

^b Different lowercase letters in the same column and uppercase letters in the same row represent significant differences (Fisher, P < 0.05).

^c MET: Diabetic + MET (500 mg/kg b.w.); ISO: Diabetic + ISO (1.9 mg/kg b.w.); EEEs: Diabetic + EEEs (400 mg/kg b.w.); MEEs: Diabetic + MEEs (284.7 mg/kg b.w.).

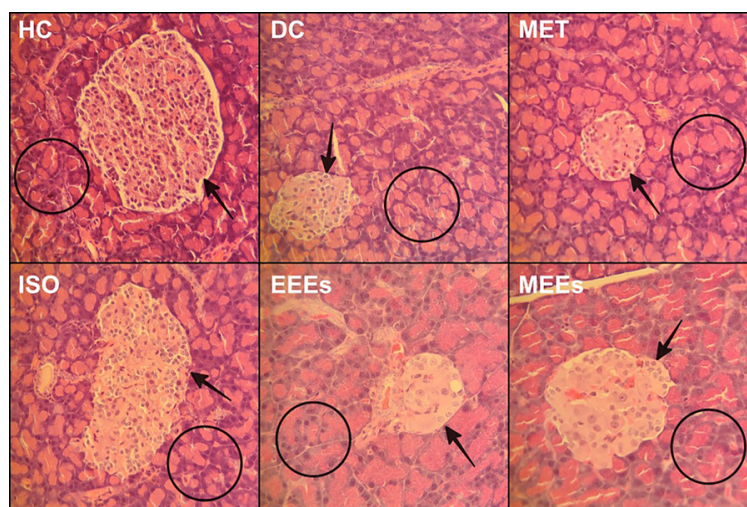


Figure 2. Histological analysis of pancreas from healthy and diabetic rats. Optical micrographs of pancreas sections from the different study groups stained with hematoxylin and eosin (40X). Diabetic + metformin (MET) [500 mg/kg b.w.]; diabetic + isorhamnetin (ISO) [1.9 mg/kg b.w.]; diabetic + ethanol extract of *Echeveria subrigida* (EEEs) [400 mg/kg b.w.]; diabetic + methanol extract of *E. subrigida* (MEEs) [284.7 mg/kg b.w.]. Islets of langerhans (arrows); acinar cells (delimited by the circle). HC, healthy control; DC, diabetic control.

4.10. Effect of the *Echeveria* Extracts on the Transcriptional Expression of SREBP-1c and PPAR α in the Liver

The transcription factor SREBP-1c activates the expression of glycolytic and lipogenic enzymes. The liver samples of the DC, EEEs, and MEEs groups expressed the SREBP-1c transcript (Figure 5). On the other hand, the transcription factor PPAR α regulates peroxisomal fatty acid β -oxidation, glucose metabolism,

and insulin sensitivity. PPAR α was only detected in the HC group (Figure 5).

5. Discussion

5.1. Body Weight

Obesity is a risk factor for developing DM2, but patients often lose weight after the disease is established (19). Therefore, body weight control is crucial in the management of DM2. Metformin is a first-

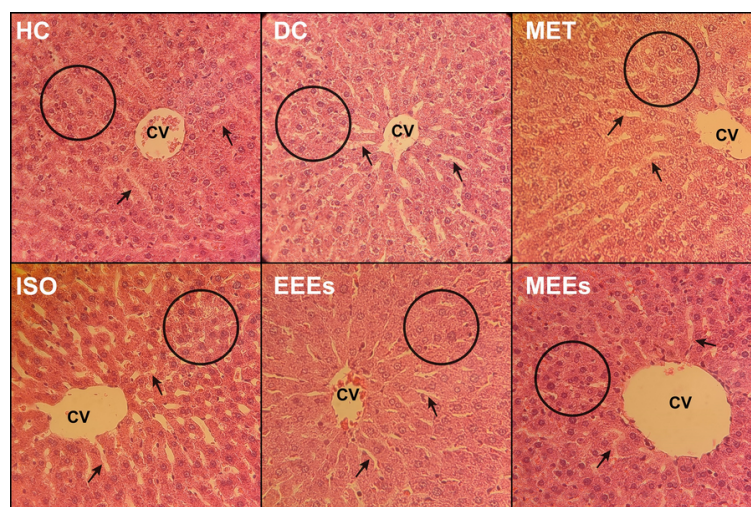


Figure 3. Histological analysis of liver from healthy and diabetic rats. Optical micrographs of liver sections from the different study groups stained with hematoxylin and eosin (40X). Diabetic + metformin (MET) [500 mg/kg b.w.]; diabetic + isorhamnetin (ISO) [1.9 mg/kg b.w.]; diabetic + ethanol extract of *Echeveria subrigida* (EEEs) [400 mg/kg b.w.]; diabetic + methanol extract of *E. subrigida* (MEEs) [284.7 mg/kg b.w.]. Sinusoids (arrows); liver parenchyma (delimited by the circle). HC, healthy control; DC, diabetic control; CV, central vein.

line treatment for DM2; it increases insulin sensitivity in peripheral tissues and decreases hyperinsulinism, hyperglycemia, and adipose tissue exposure to insulin. Consequently, MET contributes to body weight control in DM2 patients (20). These effects were observed in the present study. The body weight of the DM2 groups (DC, MET, ISO, EEEs, and MEEs) was significantly lower than that of the HC group. The mean value of the MET group was statistically higher than those of other DM2 groups but was similar to that of the EEEs group (Table 2). These results agree with the adaptogenic activity reported for the hydroalcoholic extract of *E. subrigida* in normoglycemic mice; the body weight of treated animals was lower than that of the stressed ones without changing the glucose levels (14).

5.2. Glucose Levels

The rats in the MET and MEEs groups significantly decreased their glucose levels within the first week of treatment (Table 3); these treatments showed the lowest values throughout the study. However, the glucose values for the MEEs and EEEs groups were statistically similar throughout the experiment. The glycemic control observed in the MET group aligns with previous reports. Mice treated with 400 mg/kg body weight (b.w.) of MET showed decreased hyperglycemia in the glucose tolerance test, an effect associated with decreased

intestinal absorption (21). Additionally, mice treated with pharmacologic concentrations of MET (75 μ M) showed reduced gluconeogenesis and increased ATP production (22). *Echeveria subrigida* contains compounds with α -glucosidase inhibitory activity, such as I3G, Q3G, and proanthocyanidins, which could decrease intestinal glucose absorption (13). Furthermore, Heredia-Mercado et al. (15) reported the antihyperglycemic effect of EEEs in normoglycemic mice. The effects of the mentioned compounds have been associated with different mechanisms. Persimmon tannins inhibit α -glucosidase ($IC_{50} = 0.35$ mg/mL) and α -amylase ($IC_{50} = 0.24$ mg/mL), and at 0.20 μ g/mL, they decrease glucose absorption by Caco-2 cells, likely through interaction with the SGLT1 and GLUT2 transporters (23). Quercetin (0.1 and 10 nM) and ISO (10 nM) increase glucose assimilation by L6 myotubes through increased GLUT4 translocation, similar to the positive control insulin (100 nM) (18). In pancreatic β -cells (INS-1), Q3G more effectively induces insulin release than I3G (24). In the present study, the DC and ISO groups showed the highest glucose levels throughout the experiment (Table 3). In contrast, Matboli et al. (25) reported that Wistar rats treated with ISO (40 mg/kg b.w.) under fasting conditions showed lower levels of glucose, insulin, and HOMA-IR. This effect was not observed in the present study, which may be due to the

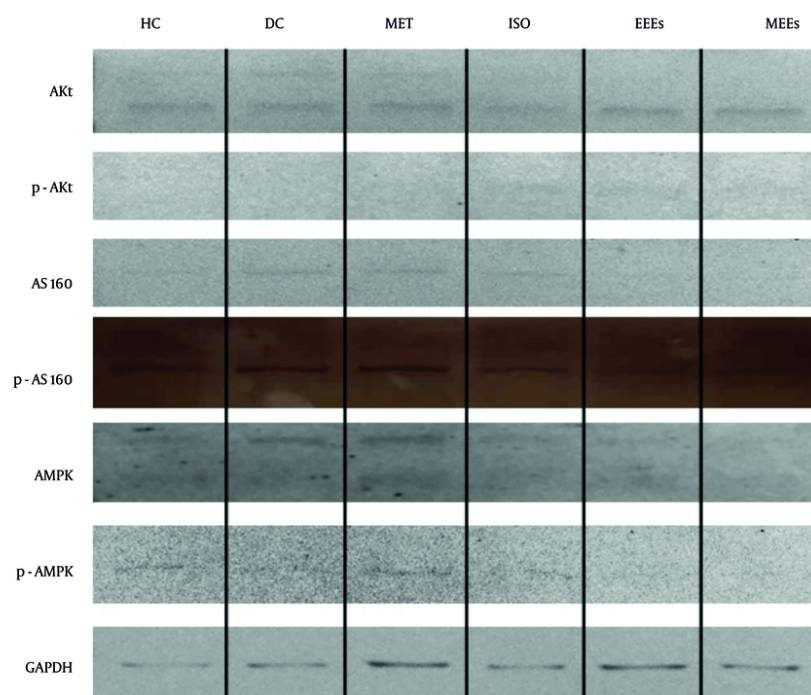


Figure 4. Western blot analysis of protein phosphorylation levels of the PI3K and AMPK signaling pathway in livers from the different study groups. Diabetic + metformin (MET) [500 mg/kg b.w.]; diabetic + isorhamnetin (ISO) [1.9 mg/kg b.w.]; diabetic + ethanol extract of *Echeveria subrigida* (EEEs) [400 mg/kg b.w.]; diabetic + methanol extract of *E. subrigida* (MEEs) [284.7 mg/kg b.w.]. HC, healthy control; DC, diabetic control.

lower concentration of ISO used (1.9 mg/kg b.w.); this dose was selected to match the I3G concentration in the EEs extract that showed *in vivo* hypoglycemic activity. At the end of the experiment, the MET, EEs, and MEEs groups reached glycemic levels similar to those of the HC group, corroborating the hypoglycemic effect of the *E. subrigida* extracts. These results indicate that EEs and MEEs contain, in addition to I3G, other compounds with additive or synergistic hypoglycemic activity. Methanolic had a better effect on glycemic control than EEs, and this extract also had higher tannin content, suggesting these compounds may be contributing to the hypoglycemic effect.

5.3. Glucose Tolerance Test

This assay corroborated the antihyperglycemic effect of EEs and MEEs, which showed patterns similar to those of the MET group (Table 4). The antihyperglycemic effect of EEs was also observed in normoglycemic mice (15). In fasted mice with STZ-induced diabetes, treatment with a flavonoid-rich *W. sinensis* extract decreased

glucose levels and increased glucose tolerance, showing a lower area under the curve (AUC) than mice in the DC group (9).

5.4. Leptin in Serum

The hormone leptin stimulates the sensation of satiety, and DM2 patients show lower leptin levels (7). Rats in the DM2 groups, except for MEEs, showed lower leptin levels than those in the HC group. All treatments increased leptin concentration compared with the DC group, and this effect was significantly higher in the EEs and MEEs groups (Table 5). Therefore, treatments with *Echeveria* extracts contribute to body weight control. Different studies have related high leptin levels to the benefits of controlling obesity and diabetes. Mice on a high-fat diet showed hyperglycemia, hyperinsulinism, increased gluconeogenesis, and decreased leptin levels; treatment with 50 mg/kg body weight (b.w.) of MET improved these conditions (22). Lipodystrophic and obese mice (*ob/ob*) showed hyperinsulinism and increased levels of SREBP-1c,

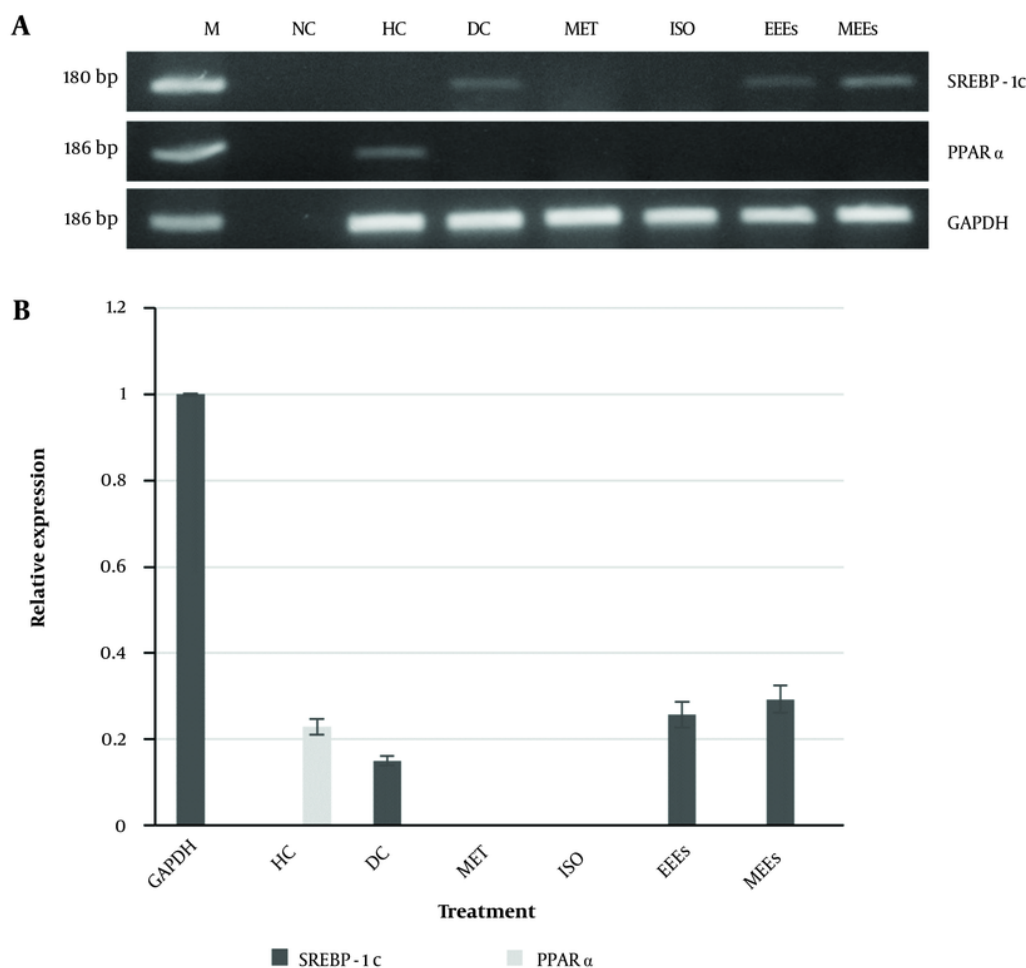


Figure 5. A, gene expression analysis of SREBP-1c and PPAR α by RT-PCR; B, relative expression of SREBP-1c and PPAR α . Diabetic + metformin (MET) [500 mg/kg b.w.]; diabetic + isorhamnetin (ISO) [1.9 mg/kg b.w.]; diabetic + ethanol extract of *Echeveria subrigida* (EEes) [400 mg/kg b.w.]; diabetic + methanol extract of *E. subrigida* (MEes) [284.7 mg/kg b.w.]. M, marker; NC, negative control; HC, healthy control; DC, diabetic control.

enzymes of fatty acid synthesis, and gluconeogenesis; leptin treatment helped reduce these negative changes (8). The same authors reported that rats with STZ-induced diabetes showed lower leptin levels, which increased with insulin treatment (8).

5.5. Anti- and Pro-inflammatory Molecules

Hyperglycemia leads to the accumulation of glyceraldehyde 3-phosphate in the liver, which can be converted to diacylglycerol (DAG). The DAG activates protein kinase C (PKC), known for its proinflammatory effects, including the activation of nuclear factor kappa B (NF- κ B). Moreover, TNF- α also activates NF- κ B, which

increases the expression of the proinflammatory cytokine IL-6, stimulating the recruitment of macrophages (4, 6). Damaged hepatocytes activate Kupffer cells, inducing the release of proinflammatory molecules [cytokines (e.g., TNF- α , IL-6, TGF- β) and chemokines (e.g., MCP-1)]. Most pancreatic cells increase NF- κ B production, leading to the transcription of proinflammatory cytokine and chemokine genes. These inflammatory conditions contribute to insulin resistance and diabetes (4, 6). In this study, rats in the DC group showed increased levels of most proinflammatory and anti-inflammatory (IL-4 and IL-10) cytokines (Table 6). This apparent contradiction is

supported by a meta-analysis showing that most patients with DM2 had increased IL-10 levels (26). In another study, DM2 patients presented high levels of both proinflammatory (IL-6, IL-12, and TNF- α) and anti-inflammatory cytokines (IL-4 and IL-10) (27). Patients with DM2 showed hypo-responsiveness to IL-10. This phenomenon was corroborated by experiments on macrophages exposed to high glucose concentration (15 mM), where IL-10 treatment was less effective in inhibiting LPS-induced TNF- α production, possibly due to impaired STAT3 activation by IL-10 (28). The levels of TNF- α and IL-10 in the kidneys and sciatic nerves of diabetic rats were higher compared with non-DC rats. These effects were mitigated in diabetic rats treated with curcumin or captopril and were associated with the inhibition of the angiotensin-converting enzyme (ACE) (29). Obese and alloxan-induced diabetic rats showed higher TNF- α and IL-10 levels compared to control rats; treatment with garlic reduced TNF- α levels in both obese (20%) and diabetic rats (18.3%), and it also increased IL-10 levels in obese rats but failed to increase or maintain IL-10 levels in diabetic rats, probably due to impaired STAT3 activation by IL-10 (30). This research demonstrates that MET and *Echeveria* (EEEs and MEEs) treatments reversed the increased cytokine levels observed in DC rats, with *Echeveria* extracts showing the best results (Table 6). Previous research showed that the hydroalcoholic extract of *E. subrigida* increases mice splenocyte proliferation and inhibits oxidative stress induced by H₂O₂ in *Saccharomyces cerevisiae* (14), supporting the results of the present study.

5.6. Histological Analysis of Liver and Pancreas Tissues

The pancreas secretes insulin and glucagon, essential hormones for carbohydrate metabolism. Treating animals with STZ damages the pancreatic β -cells and induces diabetes (31). Diabetic rats on a high-fat diet show damaged pancreatic islets of the β -cells, and insulin immunoreactivity is lost. Treatment of these rats with a *W. sinensis* extract improved pancreas structure (9). In this study, the pancreas of rats treated with EEEs, MEEs, and ISO showed Langerhans islets of irregular size and shape, indicating no tissue regeneration effect (Figure 2).

In patients with untreated DM2, the liver develops progressive damage, including non-alcoholic hepatic steatosis, due to the accumulation of fat vacuoles in the hepatocyte cytoplasm (32). In this research, the liver slices showed neither steatosis nor morphologic

changes due to DM2 progression, likely because of the short time after DM2 establishment (Figure 3). In this regard, mice fed a high-fat diet for four weeks and with diabetes induced by STZ showed steatosis that decreased after treatment with the *W. sinensis* extract (9).

5.7. Activation of the PI3K and AMPK Pathways in the Liver

The liver is essential in lipid, carbohydrate, and protein metabolism, processes regulated by kinases such as PI3K and AMPK (4, 33). AMPK is a cellular energy sensor that activates metabolic processes to produce energy while inactivating those that require energy (34). The activity of this kinase depends on the evaluated compound and metabolic context (35). For instance, treatment of primary hepatocytes with 75 μ M MET increases mitochondrial density and respiratory rate by activating AMPK. Moreover, AMPK mutant mice fed a high-fat diet are MET-resistant (22). As expected, this study showed that AMPK phosphorylation was induced by MET (Figure 4). On the other hand, diabetic rats showed higher AMPK levels and lower p-AMPK levels than healthy rats. In this regard, treating diabetic rats with an extract of *Psidium guajava* leaves increased AMPK levels, suggesting the importance of this pathway in controlling diabetes (36). The treatments with EEEs and MEEs did not induce AMPK phosphorylation (Figure 4), indicating that the antidiabetic effect of *Echeveria* extracts is associated with another metabolic pathway. The results showed that Akt was phosphorylated (Figure 4), suggesting the activation of the PI3K/Akt pathway. The p-Akt protein regulates many metabolic processes. For example, many natural products activate the PI3K/Akt pathway in the liver, increasing the synthesis of fatty acids and glycogen and decreasing gluconeogenesis and glycogenolysis. These changes are mediated by the activation of mTORC1, SREBP1c, and AS160 and the inhibition of FOXO1 and GSK3, as reviewed by Savova et al. (35). The antidiabetic effect of the *W. sinensis* extract in rats is mediated by the PI3K/Akt pathway (9). The adipose tissue of rats with diabetes induced by STZ showed decreased levels of the Akt2 transcript, and treatment with 40 mg/kg body weight (b.w.) of ISO increased the levels of this transcript (25). In L6 myotubes treated with ISO (1 and 10 nM), the increased translocation of GLUT4 was exclusively associated with the PI3K pathway (18). This result agrees with the increase in insulin delivery mediated by the PI3K/Akt pathway, induced by I3G but not by quercetin in INS-1 cells (24). On the other hand, the antidiabetic

effect of *P. guajava* leaves was associated with increased protein levels of PI3K, p-Akt, and GLUT2 (36). Therefore, this study shows that the hyperglycemia control in diabetic rats by *Echeveria* extracts (EEEs and MEEs) is associated with the PI3K/Akt pathway.

5.8. Analysis of the Transcriptional Expression of SREBP-1c and PPAR α in the Liver

The expression analysis showed that the treatment of diabetic rats with EEEs and MEEs activated the PI3K/Akt pathway (Figure 5). The Akt protein regulates the expression of the transcription factor SREBP-1c and promotes the expression of glycolytic and lipogenic enzymes (35). Reports on SREBP-1c expression have shown contrasting results (8, 37). In rats with STZ-induced diabetes, the mRNA levels of SREBP-1c decreased simultaneously with insulin levels, and the mRNA levels of glucokinase and fatty acid synthase were also reduced (8). Concurrently, there was an increase in transcript levels of gluconeogenic enzymes, such as glucose 6-phosphatase, fructose 1, 6-bisphosphatase, and phosphoenolpyruvate carboxykinase (8). Conversely, increased SREBP-1c levels were found in diabetic mice (37). This study showed the Akt protein expression in the rats of the DC group but not its phosphorylation. Despite this, the transcriptional expression of SREBP-1c in these animals indicates that hyperglycemia leads to hyperinsulinism and activation of fatty acid synthesis (35).

In the liver, the PGC1 α /PPAR α signaling pathway depends on the PI3K/Akt pathway and responds to changes in the feeding-fasting cycle. During fasting, PGC1 α /PPAR α activates the genes involved in fatty acid transport and β -oxidation (35). The function of PPAR α was demonstrated in fasted PPAR α -null mice, which showed lipid accumulation in the liver and impairments in gluconeogenesis and β -oxidation (38). Moreover, mice fed a high-fat diet showed higher transcriptional and translational expression of liver PPAR α . Therefore, PPAR α expression should be observed in groups where SREBP-1c is not expressed; however, PPAR α was only detected in the HC group because they were fasting and needed to use their energy reserves (38). The absence of PPAR α expression in the EEEs and MEEs groups could be due to their antidiabetic effects not being mediated by the AMPK pathway (39).

5.9. Conclusions

The extracts of *E. subrigida* (EEEs and MEEs) exhibited antidiabetic activity in rats, effectively limiting body weight gain and reducing hyperglycemia. The results indicate that EEEs and MEEs inhibit gluconeogenesis and glycogenolysis while promoting fatty acid synthesis in the liver. These effects are likely due to a reduction in pro-inflammatory cytokine serum levels and the positive regulation of the PI3K/Akt pathway in the liver, which affects the transcriptional expression of SREBP-1c and PPAR α . Consequently, extracts of *E. subrigida* may be developed into food supplements or pharmaceutical preparations for the prevention or treatment of obesity and DM2.

Footnotes

Authors' Contribution: F. D. V., R. P. U., J. A. L. V., G. L. P., and G. L. A. contributed to the study design and data analysis. Y. E. Z., R. P. U., J. G. R. Q., M. S. D. P., K. V. P. H., and G. L. A. performed experiments and analyzed data. Y. E. Z., F. D. V., and G. L. A. wrote the first draft manuscript. All authors reviewed the manuscript and approved its final form for publication.

Conflict of Interests Statement: The authors declared no conflict of interest.

Data Availability: The data presented in this study are uploaded during submission and are openly available for readers upon request.

Ethical Approval: The animal management was carried out according to the Official Mexican Standard NOM-062-ZOO-1999, and the protocol was approved by the Ethical Committee of the School of Veterinary Medicine and Zootechnics of Autonomous University of Sinaloa (approval number 33/0521).

Funding/Support: The National Council for Humanities, Science, and Technology of Mexico (CONAHCYT) funded this research (A1-S-24537) and provided a scholarship to Yudith Escobar-Zuñiga.

References

- Magliano DJ, Boyko EJ. *IDF Diabetes Atlas Brussels*. Brussels, Belgium: Int Diabet Fed; 2021. Available from: <https://diabetesatlas.org/>.
- World Health Organization. *Diabetes*. Geneva, Italy: World Health Org; 2023. Available from: <https://www.who.int/news-room/fact-sheets/detail/diabetes>.
- Gutierrez-Rodelo C, Roura-Guiberna A, Olivares-Reyes JA. [Molecular Mechanisms of Insulin Resistance: An Update]. *Gac Med Mex*.

- 2017;**153**(2):214-28. ES. [PubMed ID: [28474708](#)].
4. Mobasheri L, Ahadi M, Beheshti Namdar A, Alavi MS, Bemidinezhad A, Moshirian Farahi SM, et al. Pathophysiology of diabetic hepatopathy and molecular mechanisms underlying the hepatoprotective effects of phytochemicals. *Biomed Pharmacother*. 2023;**167**:115502. [PubMed ID: [37734266](#)]. <https://doi.org/10.1016/j.biopha.2023.115502>.
 5. Babu PV, Liu D, Gilbert ER. Recent advances in understanding the anti-diabetic actions of dietary flavonoids. *J Nutr Biochem*. 2013;**24**(11):1777-89. [PubMed ID: [24029069](#)]. [PubMed Central ID: [PMC3821977](#)]. <https://doi.org/10.1016/j.jnutbio.2013.06.003>.
 6. Putra I, Fakhruddin N, Nurrochmad A, Wahyuono S. A Review of Medicinal Plants with Renoprotective Activity in Diabetic Nephropathy Animal Models. *Life (Basel)*. 2023;**13**(2). [PubMed ID: [36836916](#)]. [PubMed Central ID: [PMC9963806](#)]. <https://doi.org/10.3390/life13020560>.
 7. Amitani M, Asakawa A, Amitani H, Inui A. The role of leptin in the control of insulin-glucose axis. *Front Neurosci*. 2013;**7**:51. [PubMed ID: [23579596](#)]. [PubMed Central ID: [PMC3619125](#)]. <https://doi.org/10.3389/fnins.2013.00051>.
 8. Shimomura I, Matsuda M, Hammer RE, Bashmakov Y, Brown MS, Goldstein JL. Decreased IRS-2 and increased SREBP-1c lead to mixed insulin resistance and sensitivity in livers of lipodystrophic and ob/ob mice. *Mol Cell*. 2000;**6**(1):77-86. [PubMed ID: [10949029](#)].
 9. Huang Y, Zhou T, Zhang Y, Huang H, Ma Y, Wu C, et al. Antidiabetic activity of a Flavonoid-Rich extract from flowers of *Wisteria sinensis* in type 2 diabetic mice via activation of the IRS-1/PI3K/Akt/GLUT4 pathway. *J Func Foods*. 2021;**77**. <https://doi.org/10.1016/j.jff.2020.104338>.
 10. López-Angulo G, Montes-Avila J, Díaz-Camacho SP, Vega-Aviña R, Báez-Flores ME, Delgado-Vargas F. Bioactive components and antimutagenic and antioxidant activities of two *Echeveria* DC. species. *Indust Crops Products*. 2016;**85**:38-48. <https://doi.org/10.1016/j.indcrop.2016.02.044>.
 11. Lopez-Angulo G, Montes-Avila J, Diaz-Camacho SP, Vega-Avina R, Lopez-Valenzuela JA, Delgado-Vargas F. Comparison of terpene and phenolic profiles of three wild species of *Echeveria* (Crassulaceae). *J Appl Bot Food Qual*. 2018;**91**:145-54.
 12. Lopez-Angulo G, Montes-Avila J, Díaz-Camacho SP, Vega-Aviña R, Ahumada-Santos YP, Delgado-Vargas F. Chemical composition and antioxidant, α -glucosidase inhibitory and antibacterial activities of three *Echeveria* DC. species from Mexico. *Ar J Chem*. 2019;**12**(8):1964-73. <https://doi.org/10.1016/j.arabjc.2014.11.050>.
 13. Lopez-Angulo G, Miranda-Soto V, Lopez-Valenzuela JA, Montes-Avila J, Diaz-Camacho SP, Garzon-Tiznado JA, et al. α -Glucosidase inhibitory phenolics from *Echeveria subrigida* (B. L. Rob & Seaton) leaves. *Nat Prod Res*. 2022;**36**(4):1058-61. [PubMed ID: [33190551](#)]. <https://doi.org/10.1080/14786419.2020.1844695>.
 14. Lopez-Angulo G, Diaz-Camacho SP, Heredia-Mercado B, Montes-Avila J, Delgado-Vargas F. Adaptogenic, immunomodulatory, and antioxidant activities of three *Echeveria* species (Crassulaceae). *South African J Botany*. 2022;**151**:255-62. <https://doi.org/10.1016/j.sajb.2022.10.001>.
 15. Heredia-Mercado B, Delgado-Vargas F, Lopez-Valenzuela JA, Montes-Avila J, Osuna-Martinez LU, Lopez-Angulo G. Effect of a Standardized Hydroalcoholic Extract of *Echeveria subrigida* on Mice Glycemia and In Vitro Kinetics of α -Glucosidase Inhibition. *Indian J Pharmaceut Sci*. 2022;**85**(2). <https://doi.org/10.36468/pharmaceutical-sciences.1114>.
 16. Heredia-Mercado B, Delgado-Vargas F, Osuna-Martínez LU, Noguera-Corona E, Lopez-Valenzuela JA, Ramos-Payan R, et al. Antidiabetic Potential and Chronic Toxicity of Hydroalcoholic Extract of *Echeveria subrigida* Leaves. *Pharmacog Res*. 2023;**15**(2):315-27. <https://doi.org/10.5530/pres.15.2.034>.
 17. Li J, Gong F, Li F. Hypoglycemic and hypolipidemic effects of flavonoids from tatarly buckwheat in type 2 diabetic rats. *Biomed Res*. 2016;**27**(1):132-7.
 18. Jiang H, Yamashita Y, Nakamura A, Croft K, Ashida H. Quercetin and its metabolite isorhamnetin promote glucose uptake through different signalling pathways in myotubes. *Sci Rep*. 2019;**9**(1):2690. [PubMed ID: [30804434](#)]. [PubMed Central ID: [PMC6389993](#)]. <https://doi.org/10.1038/s41598-019-38711-7>.
 19. de Luis Roman D, Garrachon Vallo F, Carretero Gomez J, Lopez Gomez JJ, Tarazona Santabalbina FJ, Guzman Rolo G, et al. [La masa muscular disminuida en la diabetes de tipo 2. Una comorbilidad oculta que debemos tener en cuenta [Decreased muscle mass in type-2 diabetes. A hidden comorbidity to consider]. *Nutrición Hospitalaria*. 2023. ES. <https://doi.org/10.20960/nh.04468>.
 20. Seifarth C, Schehler B, Schneider HJ. Effectiveness of metformin on weight loss in non-diabetic individuals with obesity. *Exp Clin Endocrinol Diabet*. 2013;**121**(1):27-31. [PubMed ID: [23147210](#)]. <https://doi.org/10.1055/s-0032-1327734>.
 21. Horakova O, Kroupova P, Bardova K, Buresova J, Janovska P, Kopecky J, et al. Metformin acutely lowers blood glucose levels by inhibition of intestinal glucose transport. *Sci Rep*. 2019;**9**(1):6156. [PubMed ID: [30992489](#)]. [PubMed Central ID: [PMC6468119](#)]. <https://doi.org/10.1038/s41598-019-42531-0>.
 22. Wang Y, An H, Liu T, Qin C, Sesaki H, Guo S, et al. Metformin Improves Mitochondrial Respiratory Activity through Activation of AMPK. *Cell Rep*. 2019;**29**(6):1511-1523 e5. [PubMed ID: [31693892](#)]. [PubMed Central ID: [PMC6866677](#)]. <https://doi.org/10.1016/j.celrep.2019.09.070>.
 23. Li K, Yao F, Du J, Deng X, Li C. Persimmon Tannin Decreased the Glycemic Response through Decreasing the Digestibility of Starch and Inhibiting α -Amylase, α -Glucosidase, and Intestinal Glucose Uptake. *J Agric Food Chem*. 2018;**66**(7):1629-37. [PubMed ID: [29388426](#)]. <https://doi.org/10.1021/acs.jafc.7b05833>.
 24. Lee D, Park J, Lee S, Kang K. In Vitro Studies to Assess the α -Glucosidase Inhibitory Activity and Insulin Secretion Effect of Isorhamnetin 3-O-Glucoside and Quercetin 3-O-Glucoside Isolated from *Salicornia herbacea*. *Processes*. 2021;**9**(3). <https://doi.org/10.3390/pr9030483>.
 25. Matboli M, Saad M, Hasanin AH, Saleh LA, Baher W, Bekhet MM, et al. New insight into the role of isorhamnetin as a regulator of insulin signaling pathway in type 2 diabetes mellitus rat model: Molecular and computational approach. *Biomed Pharmacother*. 2021;**135**:111176. [PubMed ID: [33401224](#)]. <https://doi.org/10.1016/j.biopha.2020.111176>.
 26. Zi C, He L, Yao H, Ren Y, He T, Gao Y. Changes of Th17 cells, regulatory T cells, Treg/Th17, IL-17 and IL-10 in patients with type 2 diabetes mellitus: a systematic review and meta-analysis. *Endocrine*. 2022;**76**(2):263-72. [PubMed ID: [35397088](#)]. <https://doi.org/10.1007/s12020-022-03043-6>.
 27. Payares NV, Vivas MC, d C Martinez A, Tascon AJ. [Niveles plasmáticos de citocinas pro y anti inflamatorias como biomarcadores de diabetes mellitus tipo 2]. *Revista de la Federación Argentina de Cardiología*. 2023;**52**(3):122-8. ES.
 28. Barry JC, Shakibakho S, Durrer C, Simtchouk S, Jawanda KK, Cheung ST, et al. Hyporesponsiveness to the anti-inflammatory action of interleukin-10 in type 2 diabetes. *Sci Rep*. 2016;**6**:21244. [PubMed ID: [26883847](#)]. [PubMed Central ID: [PMC4756700](#)]. <https://doi.org/10.1038/srep21244>.
 29. Abd Allah ES, Gomaa AM. Effects of curcumin and captopril on the functions of kidney and nerve in streptozotocin-induced diabetic

- rats: role of angiotensin converting enzyme 1. *Appl Physiol Nutr Metab.* 2015;**40**(10):1061-7. [PubMed ID: 26398443]. <https://doi.org/10.1139/apnm-2015-0145>.
30. Hashem RM, Mahmoud MF, El-Moselhy MA, Soliman HM. Interleukin-10 to tumor necrosis factor-alpha ratio is a predictive biomarker in nonalcoholic fatty liver disease: interleukin-10 to tumor necrosis factor-alpha ratio in steatohepatitis. *Eur J Gastroenterol Hepatol.* 2008;**20**(10):995-1001. [PubMed ID: 18787467]. <https://doi.org/10.1097/MEG.0b013e3282fd6f65f>.
31. Furman BL. Streptozotocin-Induced Diabetic Models in Mice and Rats. *Curr Protoc.* 2021;**1**(4). e78. [PubMed ID: 33905609]. <https://doi.org/10.1002/cpz1.78>.
32. Dharmalingam M, Yamasandhi PG. Nonalcoholic Fatty Liver Disease and Type 2 Diabetes Mellitus. *Indian J Endocrinol Metab.* 2018;**22**(3):421-8. [PubMed ID: 30090738]. [PubMed Central ID: PMC6063173]. https://doi.org/10.4103/ijem.IJEM_585_17.
33. Alamri ZZ. The role of liver in metabolism: An updated review with physiological emphasis. *Int J Basic Clin Pharmacol.* 2018;**7**(11). <https://doi.org/10.18203/2319-2003.ijbcp20184211>.
34. Wauman J, Tavernier J. Leptin receptor signaling: pathways to leptin resistance. *Front Biosci (Landmark Ed).* 2011;**16**(7):2771-93. [PubMed ID: 21622208]. <https://doi.org/10.2741/3885>.
35. Savova MS, Mihaylova LV, Tews D, Wabitsch M, Georgiev MI. Targeting PI3K/AKT signaling pathway in obesity. *Biomed Pharmacother.* 2023;**159**:114244. [PubMed ID: 36638594]. <https://doi.org/10.1016/j.biopha.2023.114244>.
36. Vinayagam R, Jayachandran M, Chung SSM, Xu B. Guava leaf inhibits hepatic gluconeogenesis and increases glycogen synthesis via AMPK/ACC signaling pathways in streptozotocin-induced diabetic rats. *Biomed Pharmacother.* 2018;**103**:1012-7. [PubMed ID: 29710658]. <https://doi.org/10.1016/j.biopha.2018.04.127>.
37. Shimomura I, Bashmakov Y, Horton JD. Increased levels of nuclear SREBP-1c associated with fatty livers in two mouse models of diabetes mellitus. *J Biol Chem.* 1999;**274**(42):30028-32. [PubMed ID: 10514488]. <https://doi.org/10.1074/jbc.274.42.30028>.
38. Kersten S, Seydoux J, Peters JM, Gonzalez FJ, Desvergne B, Wahli W. Peroxisome proliferator-activated receptor alpha mediates the adaptive response to fasting. *J Clin Invest.* 1999;**103**(11):1489-98. [PubMed ID: 10359558]. [PubMed Central ID: PMC408372]. <https://doi.org/10.1172/JCI6223>.
39. Grabacka M, Pierzchalska M, Dean M, Reiss K. Regulation of Ketone Body Metabolism and the Role of PPARalpha. *Int J Mol Sci.* 2016;**17**(12). [PubMed ID: 27983603]. [PubMed Central ID: PMC5187893]. <https://doi.org/10.3390/ijms17122093>.